Biomedicine & Pharmacotherapy 157 (2023) 114060

Contents lists available at ScienceDirect

Biomedicine & Pharmacotherapy

journal homepage: www.elsevier.com/locate/biopha

SOCS2 protects against chemical-induced hepatocellular carcinoma progression by modulating inflammation and cell proliferation in the liver

Juan José Cabrera-Galván [a,b], Eduardo Araujo [b], Mercedes de Mirecki-Garrido [a], David Pérez-Rodríguez [a], Borja Guerra [a,c], Haidée Aranda-Tavío [a], Miguel Guerra-Rodríguez [a], Yeray Brito-Casillas [a], Carlos Melián [a], María Soledad Martínez-Martín [a,b,d], Leandro Fernández-Pérez [a,c], Carlota Recio [a,*,1]

[a] Instituto Universitario de Investigaciones Biomédicas y Sanitarias (IUIBS), Universidad de Las Palmas de Gran Canaria (ULPGC), Las Palmas de Gran Canaria, Spain
[b] Departamento Morfología, Instituto Universitario de Investigaciones Biomédicas y Sanitarias (IUIBS), Universidad de Las Palmas de Gran Canaria (ULPGC), Las Palmas de Gran Canaria, Spain
[c] Unidad de Biomedicina (Unidad Asociada al CSIC), Instituto Universitario de Investigaciones Biomédicas y Sanitarias (IUIBS), Universidad de Las Palmas de Gran Canaria, Las Palmas de Gran Canaria, Spain and Instituto de Investigaciones Biomédicas "Alberto Sols" Consejo Superior de Investigaciones Científicas-Universidad Autónoma de Madrid, Madrid, Spain
[d] Servicio Anatomía Patológica, Complejo Hospitalario Universitario Insular - Materno Infantil, Las Palmas de Gran Canaria, Spain

ARTICLE INFO

Keywords:
Hepatocellular carcinoma
SOCS2
STAT
Inflammation
Therapeutic target
Biomarker

ABSTRACT

Hepatocellular carcinoma (HCC) is one of the most prevalent and lethal cancers worldwide, but the precise intracellular mechanisms underlying the progression of this inflammation associated cancer are not well established. SOCS2 protein plays an important role in the carcinogenesis of different tumors by regulating cytokine signalling through the JAK/STAT axis. However, its role in HCC is unclear. Here, we investigate the role of SOCS2 in HCC progression and its potential as HCC biomarker. The effects of SOCS2 in HCC progression were evaluated in an experimental model of diethylnitrosamine (DEN)-induced HCC in C57BL/6 and SOCS2 deficient mice, in cultured hepatic cells, and in liver samples from HCC patients. Mice lacking SOCS2 showed higher liver tumor burden with increased malignancy grade, inflammation, fibrosis, and proliferation than their controls. Protein and gene expression analysis reported higher pSTAT5 and pSTAT3 activation, upregulation of different proteins involved in survival and proliferation, and increased levels of proinflammatory and pro-tumoral mediators in the absence of SOCS2. Clinically relevant, downregulated expression of SOCS2 was found in neoplasia from HCC patients compared to healthy liver tissue, correlating with the malignancy grade. In summary, our data show that lack of SOCS2 increases susceptibility to chemical-induced HCC and suggest the tumor suppressor role of this protein by regulating the oncogenic and inflammatory responses mediated by STAT5 and STAT3 in the liver. Hence, SOCS2 emerges as an attractive target molecule and potential biomarker to deepen in the study of HCC treatment.

1. Introduction

Hepatocellular carcinoma (HCC) is a deadly human malignancy with high incidence worldwide, being the most common form of liver cancer responsible for 90 % of the primary malignant liver tumors in adults [1,2]. Advanced HCC has poor prognosis and small survival rates since surgery and chemotherapy are effective in a low percentage of patients [3]. However, recent studies have demonstrated that targeted molecular therapies result promising in the treatment for HCC in appropriated selected patients, although they still show limitations [3,4]. Therefore, new insights into the molecular mechanisms of HCC progression as well as the identification of new molecular targets and biomarkers to develop novel strategies for its prognosis and treatment are urgently required.

Accumulating epidemiological and clinical studies have provided

* Correspondence to: Universidad de Las Palmas de Gran Canaria (ULPGC), Instituto Universitario de Investigaciones Biomédicas y Sanitarias (IUIBS), Paseo Blas Cabrera Felipe "Físico", 17, 35016 Las Palmas, Spain.
E-mail address: carlota.recio@ulpgc.es (C. Recio).
[1] ORCID 0000-0002-8832-2826.

https://doi.org/10.1016/j.biopha.2022.114060
Received 24 August 2022; Received in revised form 3 November 2022; Accepted 27 November 2022
Available online 28 November 2022

evidence that HCC is closely linked to chronic inflammation, which favours the initial genetic alterations that give rise to cancer cells, establishes a tissue microenvironment that allows the tumor to progress and metastasize, and activates immunosuppressive mechanisms that prevent an effective immune response against the tumor [5,6]. Liver resident inflammatory cells actively contribute to hepatic damage during HCC, being mainly activated by apoptotic hepatocytes and producing a wide range of inflammatory cytokines (TNFα and IL-6, among others), reactive oxygen species, and growth controlling factors that participate in tumor progression [7]. The activation of the inflammatory response leads the recruitment of new immune cells, mainly monocytes and neutrophils, which infiltrate into the liver and perpetuate the inflammatory burden, inducing the compensatory uncontrolled proliferation of surviving hepatocytes [8]. In addition, as result of an inaccurate regulation, key inflammatory signalling pathways are hyperactivated in HCC, contributing to angiogenesis, differentiation, proliferation, and survival of liver cancer cells [9–11]. Current targeted therapies that do not involve surgical treatment or transplant are addressed towards key phases in carcinogenic signalling pathways in order to restrain systemic toxicity. However, there is not a recognized predominant signalling cascade linked to hepatocarcinogenesis [9].

Suppressor of cytokine signalling (SOCS) proteins are leading negative regulators of cytokine signalling mediated by the Janus kinase / Signal Transducer and Activator of Transcription (JAK/STAT) signalling pathway [12]. JAK/STAT modulates processes such as cell proliferation, differentiation, migration, and apoptosis, among others. Under physiological conditions, JAK/STAT activation is strictly regulated, making its activity rapid and transient [13]. However, aberrant STAT hyperactivation has been reported in several pathologies including cancer, leading to uncontrolled cell proliferation, oncogenic transformation, tumor cell invasion, and metastasis [13]. In many cases, STAT constitutive activation is the result of a dysfunction in the negative regulation of the pathway. In fact, abnormal expression of SOCS proteins has been discovered in several tumor types, not only in cancer cells but also in immune cells in the tumor microenvironment [14–16]. Among the eight members of the SOCS family, the involvement of SOCS1 and SOCS3 has been extensively investigated in the context of cancer, and both tumor suppressive and oncogenic roles have been reported [17,18]. Likewise, SOCS2 has been attributed key regulative roles in the carcinogenesis of different types of cancer [19,20]. Previous studies have demonstrated that low SOCS2 expression levels are linked to a poor prognosis and higher tumor progression in breast, ovarian, prostate, lung, and hematological malignancies [21–25]. Furthermore, SOCS2 has been validated as an effective biomarker in colorectal cancer, where it exhibits a key value in the early disease prognosis [26]. In experimental models, SOCS2 deletion has been shown to promote the spontaneous progression of intestinal tumors, whereas its overexpression inhibits the proliferation of colon cancer cells [27].

In the liver, the axis JAK2/STAT5/SOCS2 controls Growth Hormone (GH) signalling, being its correct functioning vital for an adequate hepatocyte physiology [28]. To date, very few studies have investigated the role of SOCS2 in liver cancer. Available reports suggest an indirect link between SOCS2 expression and HCC prognosis [29–31]. However, there are not mechanistic or functional studies that effectively describe the direct biological role that SOCS2 could exert in the progression of the disease. Furthermore, the phenotype of SOCS2 knockout mice regarding the liver and its associated pathologies has only been investigated in the context of hepatic steatosis, insulin resistance, and acute liver injury, but not in cancer [32,33].

Herein, the present work investigates the potential key role of SOCS2 in chemical-induced HCC with special attention in the underlying inflammatory process, in order to open the window to new therapeutic targets and novel biomarkers to improve the treatment and prognosis of this deadly disease. To that end, the progression of HCC has thoroughly been evaluated in an experimental model of diethylnitrosamine (DEN)-induced HCC in SOCS2 deficient mice and in cultured hepatic cells.

2. Methods

2.1. Mice

Animal experiments were conducted in accordance with OECD guidelines for the care and use of animals and with an approved animal protocol from the Animal Care and Use Committee of the University of Las Palmas de Gran Canaria (ULPGC, OEBA-ULPGC 11/2018).

C57BL/6 and SOCS2 knockout (referred to as SOCS2-KO or SOCS2$^{-/-}$, backcrossed to C57BL/6 background, kindly provided by P.K. Lund laboratory [34] and further breaded at ULPGC) were housed four or five to a cage, maintained under standard laboratory conditions (12-hour light/dark cycle) with food and water provided *ad libitum,* at ULPGC Animal Unit. Genotyping was performed on mice genomic DNA from a small piece of tissue by conventional PCR using Taq DNA polymerase, and PCR reactions were carried out with primers for *socs2* and *β-galactosidase* purchased from StabVida. PCR amplification products were loaded on a 2 % agarose gel containing ethidium bromide and visualized under UV light in the ChemiDoc XRS system (Bio-Rad).

2.2. Human samples

Experiments with human samples were conducted with approved protocol from the Ethics Committee CEIm Las Palmas:2021–406–1. Briefly, paraffin-embedded biopsies from livers from twelve HCC patients were obtained from the Biopsy archive of the Anatomical Pathology Service of the Complejo Hospitalario Insular Materno-Infantil of Las Palmas, Canary Islands Health Service.

2.3. HCC animal model

Fifteen-day-old C57BL/6 and SOCS2-KO male mice were injected intraperitoneally (i.p.) with a single dose (25 mg/kg) of DEN (Sigma-Aldrich) or Vehicle (VEH, 0.9 % NaCl). All animals were injected within a period of 2 months with the same DEN lot, ensuring best comparability between treated groups. Animal welfare, body weight, and food consumption were assessed every other day to detect any clinical sign. At 12- and 24-weeks post DEN treatment, a representative number of mice from each group were subjected to ultrasound assessment to potentially detect the initial tumor formation without euthanasia, using a LOGIQ P5 Ultrasound System (GE Healthcare) with a linear transducer (3–11 MHz). Body composition (lean, fat and fluid) was investigated at the initial and final points of the experiment, using a Time Domain Nuclear Magnetic Resonance Scan (Bruker Minispec LF90, Bruker Optics). The last day of the study, mice were placed in metabolic cages for 24 h to monitor their metabolic activity (urine and feces volume, water, and food consumption). After 24-(early lesions) and 48- (advanced lesions) weeks post DEN administration, animals were euthanized by isoflurane overdose, blood samples were collected, and tissues were saline-perfused for subsequent harvesting and analysis. For macroscopic evaluation, livers were removed, weighed, photographed, and externally visible tumors ($\geq$ 0.5 mm) were counted and measured. Part of the liver tissue was used for histology and immunohistochemistry, and the remaining liver samples were stored at − 80ºC for RNA and protein isolation.

Blood samples were collected into EDTA containing tubes. Part of the blood sample was used for hematological analysis using the MS4–5 Melet Schloesing Software, whereas the rest of the sample was centrifuged to separate the serum that was analysed for biochemical parameters with the Pointcare v2 Mano Medical Software.

2.4. Histology and immunohistochemistry

For histopathology, mouse liver tissues were fixed in 4 % paraformaldehyde overnight and paraffin embedded. Human livers were already in paraffin. Paraffin-embedded livers were then cut into 4 μm

slides and stored for corresponding histology and/or immunohistochemistry. For histopathological analysis, sections were hematoxylin and eosin (H&E) stained and evaluated in a blinded manner by two independent pathologists. Signs of malignancy were determined and graded according to cell atypia, cell polymorphism, distortion of lobular architecture, broadening of trabecular structures, lobular inflammation (number of inflammatory foci/field), portal inflammation, and microgranulomas. A four-point score (0, absent; 1, low; 2, moderate; 4, marked) was added to each parameter of analysis, according with the Edmondson and Steiner Liver Hepatocellular Carcinoma Classification [35]. Results were then plotted as the mean value of each parameter for each group of mice. Liver sections were also picrosirius-red stained for fibrosis detection and quantification. Immunohistochemical staining was performed using standard protocols. Briefly, slides were deparaffined at 60 ºC, 30 min, followed by xylol immersion 10 min, and hydration with decreasing ethanol concentrations up to a final distilled water bath. Sections were then treated for hot induced antigen retrieval with pH 6 citrate buffer at 95 ºC for 30 min. After washing, samples were incubated with 3 % H_2O_2-methanol 30 min for inhibition of endogenous peroxidase activity and were then blocked with 5 % Bovine Serum Albumin (BSA) in PBS containing 6 % of total serum for 1 h. Primary antibodies (anti- alpha-fetoprotein (AFP, Sigma Aldrich), anti- proliferating cell nuclear antigen (pCNA, Santa Cruz Biotechnology), anti-F4/80 (Cell Signalling), and anti-SOCS2 (Santa Cruz Biotechnology)) were then added and incubated overnight at 4 ºC. After washing, sections were incubated with HRP-conjugated anti-mouse or anti-rabbit secondary antibodies (Dako) for 30 min, followed by 5 min treatment with the diamonobenzidine (DAB) peroxidase substrate chromogen (Dako). Finally, sections were H&E counterstained, dehydrated with rising ethanol concentrations, and mounted with DPX mounting media (Sigma Aldrich). Mounted slides were observed under a microscope and photographed for quantification and imaging. The positive staining was quantified using the ImageJ software (Media Cybernetics, Inc.), and expressed by the percentage of positive cells *versus* the total number of cells per field, or the percentage of positive stained area *versus* total area, of ten high-power fields per section.

2.5. Cell isolation and culture

Mouse primary hepatocytes and liver macrophages were isolated from 12 to 15-week-old C57BL/6 and SOCS2-KO male mice as described [36]. Briefly, mouse livers were perfused by canulation of the inferior cava vein with warm (42 ºC) Hank's Balanced Salt Solution supplemented with 25 mM HEPES and 0.5 mM EDTA, at 2 mL/min. Immediately, livers were digested with 25 μg/mL Liberase (Sigma Aldrich) resuspended in warm (42 ºC) DMEM high glucose media supplemented with 1 % penicillin/streptomycin (P/S), 25 mM HEPES, and 10 % fetal bovine serum (FBS), at 2 mL/min. After digestion, liver was carefully transferred into a Petri dish and hepatic cells were gently released by tissue mincing. Cells were filtered through a 100 μm cell strainer and centrifuged for cell population separation. Hepatocytes in the pellet were then washed and resuspended in Williams E media containing 1 % P/S ready for plating; liver macrophages in the supernatant were transferred into a Percoll (Sigma-Aldrich) gradient (25 %−50 %), isolated by centrifugation, and cultured in RPMI media containing 10 % BSA and 1 % P/S. Viability of isolated cells was checked by trypan blue test. Cells were then treated with 100 μg/mL DEN for 24 h and protein and gene expression experiments were performed.

2.6. Protein analysis

Western Blot. Tissues were lysed by adding RIPA buffer (Thermo Fisher Scientific) supplemented with protease and phosphatase inhibitors (Thermo Fisher Scientific) followed by manual disruption. Protein concentration was determined by using a bicinchoninic acid (BCA) protein assay kit (ThermoFisher Scientific). Total protein (40–60 mg) was added to 4x Laemmli buffer (250 mM Tris-HCl, pH 6.8, 8 % SDS, 40 % glycerol, 0.004 % bromophenol blue, 20 % b-mercaptoethanol) and heated at 95 °C for 5 min. Samples were then resolved on SDS-PAGE gels (Bio-Rad) and transferred into nitrocellulose membranes (Thermo Fisher Scientific) that were blocked with 5 % milk or BSA diluted in Tris buffered saline with 0.05 % Tween 20 (TBS-T) for 1 h at room temperature, and then incubated with primary antibodies overnight at 4 °C. Next, membranes were incubated with HRP-conjugated anti-rabbit or anti-mouse secondary antibodies (Bio-Rad) for 1 h at room temperature. Protein bands were visualized by using the enhanced chemiluminescence Clarity™ Western ECL Substrate (Bio-Rad) in the ChemiDoc XRS system. Images were analyzed with the program Quantity one (Bio-Rad). β-actin was used as loading control. For successive antibody incubations using the same membrane, bound antibodies were removed with stripping buffer (ThermoFisher Scientific).

2.6.1. Immunofluorescence

Protein expression and location was also detected by immunofluorescence. Briefly, cells placed in a 4-well chamber-slide were fixed (4 % paraformaldehyde) for 10 min at RT, permeabilized (0.5 % Triton X-100 in PBS) for 10 min at 4 °C, blocked with 4 % BSA/PBS containing 6 % serum, and incubated with primary antibodies diluted in 4 % BSA/PBS, overnight at 4 °C. Cells were then incubated with the Alexa Fluor 488 (Cell Signalling) secondary antibody diluted in 4 % BSA/PBS for 1 h at RT. The fluorescent marker 4',6-diamidino-2-phenylindole (DAPI) was used for nuclear counterstaining. The slide was mounted with Fluormount-G® and cells were visualized using a confocal microscope.

2.7. Gene expression analysis

Mouse tissues were extracted with PureZOL RNA Isolation Reagent (Bio-Rad), and total RNA concentration and quality was determined with a ND-1000 spectrophotometer (Nano Drop Technologies). Complementary DNA was synthesized from 700 to 1000 ng RNA using the iScriptTM Reverse Transcription kit (BioRad) according to the manufacturer's instructions. Real-time quantitative PCR was performed using SYBR Green PCR Master mix (Applied Biosystems) and primers (*tnfα, il-6, il-1β, ccl2, inos, f4/80, pim1, cmyc, cd34, p53, gstp1, igf1,* from StabVida) in the Mx3005P Real-Time PCR System (Agilent). Cycle threshold values were obtained, and target gene expression was normalized to housekeeping gene (*36b4*). Relative expression results were plotted as mRNA expression divided by *36b4* expression, and normalized to VEH samples when convenient [37].

2.8. Statistical analysis

All quantitative data are expressed as mean ± SEM of *n* independent biological replicates. Statistical significance was performed using a Student's unpaired *t*-test, or one-way analysis of variance (ANOVA) followed by Dunnett's multiple comparison *post hoc* test (Prism 8 GraphPad Software, San Diego, CA, USA). Correlation analysis was performed using a Pearson's correlation test. Survival was analysed using the Kaplan–Meier method. A P value of < 0.05 was taken to be statistically significant.

3. Results

In this study, the role of SOCS2 was evaluated in a well stablished HCC mouse model that uses the chemical carcinogen DEN to induce hepatocellular carcinogenesis [38]. To that end, SOCS2-KO and C57BL6/J mice (as wild-type (WT) controls) were used. Before the beginning of the experimental model, mice were genotyped to ensure their genetic condition (Fig. 1**a**).

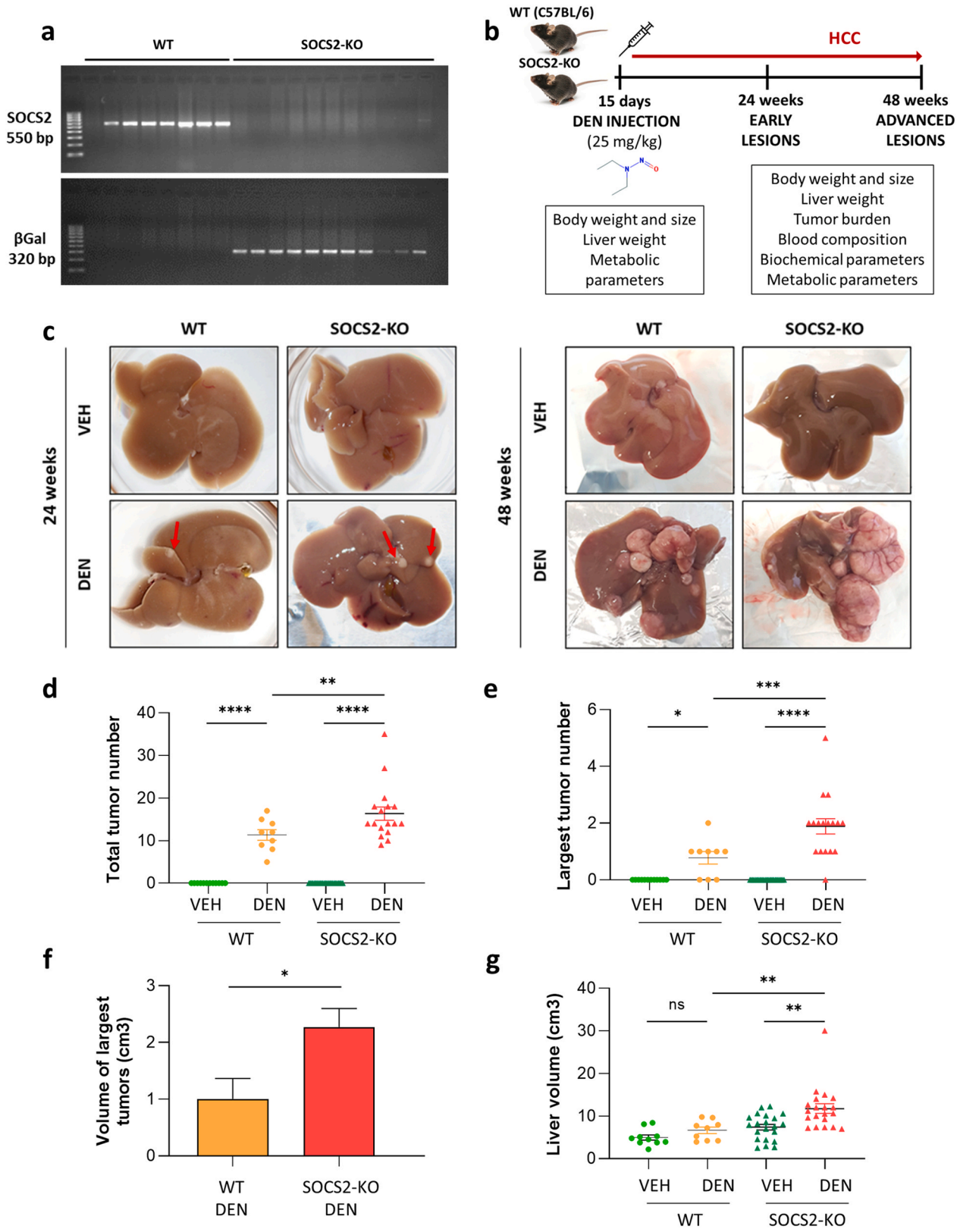

Fig. 1. Deletion of SOCS2 increases DEN-induced liver tumorigenesis. (a) Genotypic analysis of *socs2* expression in WT and SOCS2-KO mouse tissue. Small pieces of mice tissue were digested and DNA was isolated for PCR amplification with *socs2* and *β-galactosidase (β-gal)* primers. Amplification products were loaded and run on a 2 % agarose gel. (b) Experimental design of DEN-induced HCC model. (c-g) WT and SOCS2-KO male mice were given a dose of DEN (25 mg/kg) or VEH at 15 days of age and liver tissues were isolated after 24 and 48 weeks. (c) Representative images of gross liver anatomy at 24 (left) and 48 (right) weeks after VEH or DEN injection. Arrowheads indicate tumor nodules at 24 weeks. (d) Total tumor number, (e) number of largest tumors (≥ 0.5 mm), (f) volume of largest tumors, and (G) total liver volume were quantified in WT (n = 9–10) and SOCS2-KO (n = 15–20) mice 48 weeks after VEH or DEN injection. Plots represent individual values and lines represent mean values. Bars represent mean values ± SEM. Statistical significance is indicated (* $p < 0.05$, ** $p < 0.01$, *** $p < 0.001$).

3.1. Deletion of SOCS2 aggravates the development of HCC tumors in response to the chemical carcinogen DEN

To investigate the role of SOCS2 in the initiation and progression of DEN-induced carcinogenesis, SOCS2-KO mice and their WT littermates were injected 25 mg/kg DEN on day 15 after birth, and tumor formation was assessed 24 and 48 weeks later (Fig. 1b). At 24 weeks after HCC induction, only 17 % WT mice had developed nodules in the liver compared to 43 % SOCS2-KO mice, but no significant differences were found between groups regarding the total number of neoplastic formations in those tumor bearing mice. Remarkably, ultrasound assessment performed at 12 and 24 weeks led to identify a hypoechoic nodular pattern in the livers of both WT and SOCS2-KO mice and confirmed the absence of relevant differences in the number nor size of nodules between both genotypes at those early time points (Online Resource 1). However, most DEN-treated mice from both genotypes had developed macroscopically detectable neoplasia at the endpoint (48 weeks) (Fig. 1c). Interestingly, gross anatomy analysis revealed that the number and size of HCC lesions was significantly higher in DEN-treated SOCS2$^{-/-}$ mice, being the volume of largest tumors in this group more than twice compared to their WT littermates (Fig. 1d-f). Consistent with their genotype, SOCS2-KO liver volumes were significantly higher compared to those in WT mice at the study endpoint, but DEN-treated KO showed even bigger livers due to the presence of massive tumor masses (Fig. 1g).

The analysis of body weight along the study revealed that mice treated with the carcinogen start to lose weight from the last four weeks, being more pronounced in SOCS2-KO animals (Online Resource 2). However, no significant differences between DEN-treated and non-treated groups were observed in terms of body length, food intake and body composition, besides size variations associated to SOCS2$^{-/-}$ genotype [28,39] (Online Resource 2). Data gathering from metabolic cages at the end of the study showed an increased food intake by DEN-treated SOCS2-KO compared to their WT controls, and a larger volume of urine released by DEN-treated knockouts compared to their VEH-treated counterparts (Online Resource 2).

3.2. SOCS2 deficiency increases HCC liver damage, inflammation, and fibrosis during early and advanced tumor promotion

To further evaluate the impact of SOCS2 absence on tumor anatomy, a histopathological analysis was performed. H&E staining revealed that SOCS2 deficiency drastically increased malignancy of liver tumors. Histological differences between groups at 24 weeks were remarkably emphasized at 48 weeks after DEN treatment, as evidenced by all the parameters evaluated (Fig. 2a-b). As expected, control livers from VEH-treated mice contained no dysplastic lesions in both genotypes. Cell atypia, cell polymorphism, distortion of lobular architecture, and broadening of trabecular structures were analysed as features of liver malignancy, resulting in significantly higher values in DEN treated-SOCS2$^{-/-}$ mice (Fig. 2a-b). Indeed, tumor cells found in SOCS2-KO livers after 48 weeks of DEN treatment exhibited large and pleomorphic nuclei with high nuclei/cytoplasm ratios, and altered morphology compared to WT-treated mice. Furthermore, extensive architecture changes were observed in DEN-treated knockout mice and in lesser extent in their WT controls, including atypical ducts, tumoral lesions with basophilic trabeculae, infiltrates of neoplastic foci in the lumen of hepatic vein branches, and wide hemorrhagic and necrotic areas. Accordingly, DEN-treated SOCS2-KO mice were found to bear more inflammatory burden tumors than their WT controls, with increased lymphocyte and monocyte infiltration both in the lobular and portal areas (Fig. 2a-b). Notably, no relevant differences were observed in both animal groups treated with VEH. After an accurate evaluation, and according to the World Health Organization (WHO)'s description for HCC histologic patterns, the pathologist reported a predominant trabecular carcinoma histologic pattern in most of the mouse tumors within the study, followed by a solid pattern, and with only some exceptional cases of acinar cell carcinoma. As another parameter of liver damage, fibrosis was evaluated in the hepatic tissue after 48 weeks of DEN treatment. As shown in Fig. 2c-d, the morphometric analysis of Sirius Red staining brought out that SOCS2$^{-/-}$ mice exhibited more collagen bundles and therefore more fibrotic hepatic extracellular matrix than their controls. Remarkably, the analysis of the hepatic transaminases aspartate aminotransferase (AST) and alanine aminotransferase (ALT) present in mice serum revealed that DEN-treated mice showed significantly higher levels of both enzymes compared to their VEH-treated counterparts, being slightly higher in the knockout group (Fig. 2e). Furthermore, other biochemical parameters including total cholesterol and triglycerides were evaluated with no relevant differences between groups apart from the notable enhancement of total cholesterol levels observed in both WT and SOCS2-KO mice after 48 weeks of DEN treatment (Online Resource 3). Additionally, the study of mouse blood cell populations showed that the total number of white blood cells in DEN-treated WT and SOCS2$^{-/-}$ mice was significantly higher than in their counterparts, with no significant differences found in the remaining hemogram. Moreover, a reduction in the number of circulating monocytes was observed in animals treated with the carcinogen when compared to VEH-treated ones, that was more substantial in knockout mice (Online Resource 3).

3.3. SOCS2 knockout mice exhibit increased levels of HCC diagnostic markers with higher compensatory hepatocyte proliferation and leukocyte infiltration in the liver

To better characterize some key tumor features and composition, a series of immunohistochemical stains were performed in mouse liver sections from SOCS2-KO and WT mice after 48 weeks of treatment. Interestingly, the analysis and quantification of AFP staining showed that the single injection of DEN to fifteen-day-old mice resulted in the induction of AFP-expressing HCC, with significantly higher levels in the SOCS2-KO group when compared to WT controls (Fig. 3a). Furthermore, liver sections were verified by pCNA staining for the analysis of cell proliferation. As shown in Fig. 3b, SOCS2-KO mice given DEN exhibited the highest proliferative rates in comparison to their VEH-treated counterparts. Likewise, the immunostaining with the macrophage marker F4/80 revealed that DEN-induced HCC was associated with a relevant increase in intrahepatic macrophages, with significant changes between both genotypes. However, positive staining area in VEH-treated mice from both treatment groups remained at low levels (Fig. 3c).

3.4. The absence of SOCS2 triggers the hyperactivation of key inflammatory, oncogenic, and proliferative intracellular signalling pathways in DEN-induced HCC

Considering that HCC is an inflammatory-linked cancer and that SOCS2 is an important regulator of cytokine and growth factor signalling, we outlined to investigate the expression of different target proteins and genes involved in the inflammatory, oncogenic, and proliferative responses during HCC. Thus, total proteins and mRNA were isolated from livers from 48-week DEN-treated mice, and expression levels were assessed by immunoblot and quantitative real time PCR, respectively. Remarkably, immunoblot analyses revealed that pSTAT5 and pSTAT3 were significantly highly induced in DEN-treated SOCS2-KO livers compared to their controls (VEH-treated SOCS2-KO and WT mice) (Fig. 4a). Surprisingly, low levels of pSTAT3 were found in DEN-treated WT mice, whereas no significant changes in the expression levels of the total proteins (STAT5 and STAT3) were observed (Fig. 4a). Likewise, the expression of CMYC and PIM1, two key target proto-oncogenes of STAT5 that are involved in cell cycle progression, apoptosis, and transcriptional activation, was also upregulated in SOCS2 deficient mice treated with DEN (Fig. 4b). Interestingly, the evaluation of some key proteins involved in cell proliferation, survival, and migration such as ERK, AKT, and JNK, also showed augmented phosphorylated levels in DEN-treated SOCS2-KO mice compared to the other

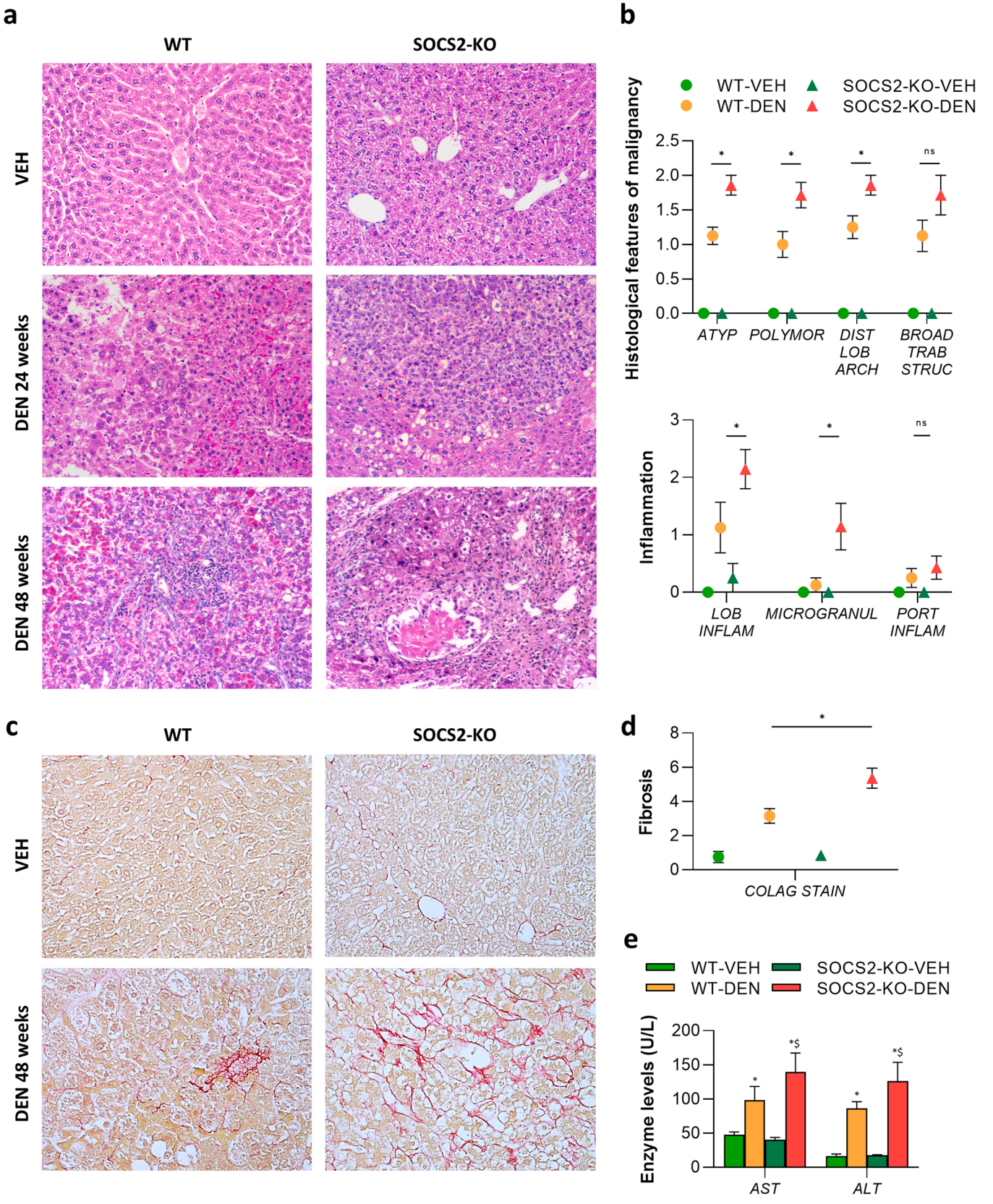

(caption on next page)

Fig. 2. SOCS2 deficiency aggravates liver damage, inflammation and fibrosis in DEN-induced HCC. WT and SOCS2-KO male mice were given a dose of DEN (25 mg/kg) or VEH at 15 days of age and liver tissues were isolated from mice after 24 and 48 weeks, paraffin-embedded and sectioned for staining and quantification. At least 10 fields from different mice were counted. (**a**) H&E staining of liver sections of WT (n = 9–10) and SOCS2-KO (n = 15–20) mice 24 and 48 weeks after VEH or DEN injection. High power (x20 magnification) representative microscopic pictures are shown. (**b**) Histological analysis of malignancy and inflammatory features in H&E sections at 48 weeks after DEN injection. ATYP, cell atypia; POLYMOR, cell polymorphism; DIST LOB ARCH, distortion lobular architecture; BROAD TRAB STRUC, broadening trabecular structure; LOB INFLAM, lobular inflammation; MICROGRANUL, microgranulomas; PORT INFLAM, portal inflammation. (**c**) Sirius red staining of liver sections of WT (n = 9–10) and SOCS2-KO (n = 15–20) mice 48 weeks after VEH or DEN injection. High power (x20 magnification) representative microscopic pictures are shown. (**d**) Positive staining (red) quantification expressed as % *vs* total area in Sirius red stained sections at 48 weeks after DEN injection. COLAG STAIN, collagen staining. (**e**) Quantification of hepatic enzyme levels in the serum of WT (n = 9–10) and SOCS2-KO (n = 15–20) mice 48 weeks after VEH or DEN injection. AST, aspartate aminotransferase; ALT, alanine aminotransferase. Plots and bars represent mean values ± SEM within each group. Statistical significance is indicated (* $p < 0.05$ *vs* WT-VEH, # $p < 0.05$ *vs* WT-DEN, $ $p < 0.05$ *vs* SOCS2-KO-VEH).

groups, without significant changes in the total protein expression levels (Fig. 4c). Full, uncropped blots can be found in **Online Resource 4**.

Regarding mRNA expression analysis, different mediators of inflammation and tumorigenicity were assessed in the HCC model. Consistently, SOCS2-KO mice given the carcinogen exhibited increased gene expression levels of the proinflammatory cytokines *tnfα*, *il-6* and *il-1β,* the macrophage chemoattractant *ccl2*, the inducible nitric oxide synthase enzyme *inos*, and the macrophage marker *f4/80*, when compared to their VEH-treated and WT counterparts (Fig. 5a). Further, the expression of the proto-oncogenes *cmyc* and *pim1*, as well as other key tumor markers in HCC such as the endothelial cell marker *cd34*, the Glutathione S-Transferase P1 (*gstp1*), and the Insulin-like growth factor-1 (*igf1*) were upregulated in the group of tumor bearing knockout mice (Fig. 5b). In contrast, mRNA levels of the tumor suppressor p53 appeared slightly downregulated in this group, although without reaching statistical significance when compared to controls (Fig. 5b). All these findings support the idea that SOCS2 deficiency favours HCC development in mice, thus suggesting that the protein may be acting as a tumor modulator in the progression of the disease.

3.5. Liver macrophages and hepatocytes lacking SOCS2 show upregulation of STAT5 and STAT3 phosphorylation levels after DEN treatment in vitro

DEN administration to mice causes several biochemical changes in the liver including the induction of hepatocyte damage and the creation of an inflammatory environment, that eventually result in the development of HCC [40]. Considering the results obtained in the liver of DEN-treated SOCS2 lacking mice, including the increased tissue damage, augmented proliferation and inflammatory cell recruitment, and enhanced expression of inflammatory markers, we wanted to elucidate whether hepatocytes, liver macrophages, or both, were responsible of these pathological changes in the absence of SOCS2 protein. Thus, liver macrophages and hepatocytes were isolated from mice and immunofluorescence assays were performed to assess the activation of pSTAT5 and pSTAT3. Of relevance, twenty-four hours post DEN treatment a noticeable increase in the activation of both transcription factors was detected in SOCS2-lacking liver macrophages, as evidenced by their almost generalized nuclear location observed in Fig. 6a. Although this activation was also patent in WT macrophages given DEN compared to their non-treated controls, there were visible differences between cells from both genotypes. Similar results were observed in liver hepatocytes, where both pSTAT5 and pSTAT3 were mainly located in the nucleus of SOCS2 knockout cells treated with the carcinogen, whereas there were some nucleus-stained cells and some cytoplasm-stained ones in DEN-treated hepatocytes from WT mice (Fig. 6b). These data suggest the important role that SOCS2 plays in the regulation of STAT signalling in both cell types, and therefore in the modulation of the inflammatory and protumoral responses in HCC.

3.6. SOCS2 as potential biomarker in human HCC

To understand the impact of SOCS2 protein and its potential prognostic relevance in human HCC, sections from liver biopsies from HCC patients were H&E stained and SOCS2 immunoassayed, and SOCS2 quantification was correlated with histopathological values within the Edmondson-Steiner scale. Likewise, sections from liver autopsies from healthy individuals were immunostained for SOCS2 and quantified. Very interestingly, liver samples from HCC patients displayed a differential pattern of SOCS2 expression depending on the tissue area, being neoplastic regions less SOCS2 -marked than non-tumoral ones (Fig. 7a-b). Furthermore, within tumoral areas of each patient, those with poorer pathological features (Edmondson-Steiner grade 3), typically showed a downregulation in SOCS2 expression. Both healthy livers and non-tumoral tissue areas surrounding neoplasia showed higher SOCS2 expression that was especially uniform and regular in the cytoplasm of hepatocytes. In contrast, neoplastic cells displayed irregular expression of SOCS2, alternating low immunostaining areas with more marked regions. Clinically relevant, these results allowed to establish a negative correlation between SOCS2 expression and HCC malignancy and suggest that SOCS2 may own a potential value as a biomarker for prognosis and/or diagnosis of human HCC (Fig. 7c). However, more samples from HCC patients would be necessary to confirm this hypothesis with stronger correlation values. Finally, Kaplan–Meier survival analysis of the HCC patient's small cohort revealed that higher levels of SOCS2 were associated with more favourable outcomes (Fig. 7d). Together, all these findings indicate that lower levels of SOCS2 expression are associated with the malignant progression of HCC.

4. Discussion

It is well-established that chronic inflammation plays a key role in the development and progression of HCC contributing to cell proliferation, angiogenesis, and metastases [9]. SOCS proteins have been implicated in the regulation of cytokines and growth factors in liver diseases, and, in particular, SOCS2 is known to play a crucial role in hepatic physiopathology [33,41,42]. Existing studies so far indirectly link SOCS2 expression with different cancer prognosis, however, its functional and mechanistic involvement in the carcinogenesis and tumor progression of HCC has been scarcely studied [16,43]. It has been shown that SOCS2 inhibits HCC metastases by regulating GH/JAK/STAT signalling pathway in hepatic cells, but little else is known [19]. In this study we delved into the impact of SOCS2 deficiency in a mouse model of DEN-induced HCC and evaluated the mechanisms by which this protein participates in HCC progression. It has been found by comparative genomic analyses that gene expression patterns seen in tumors from DEN treated mice are similar to human HCC tissue of patients with poor prognosis [44,45]. Although it is not strictly considered an inflammatory liver cancer model, DEN-induced HCC has been reported to be highly influenced by inflammatory signals [40]. Furthermore, it has been demonstrated that administration of DEN to new-born mice leads to DNA alterations by ethylation and consequently to neoplastic foci, thereby adult mice eventually develop HCC without sustained alterations of the remaining liver tissue [46]. Our data revealed that administration of 25 mg/kg DEN to fifteen-day-old mice triggered tumor formation in the mouse liver and that SOCS2 deletion increased the susceptibility to HCC after 48 weeks, evidenced by more numerous and bigger tumors. This concurs with numerous studies that have reported

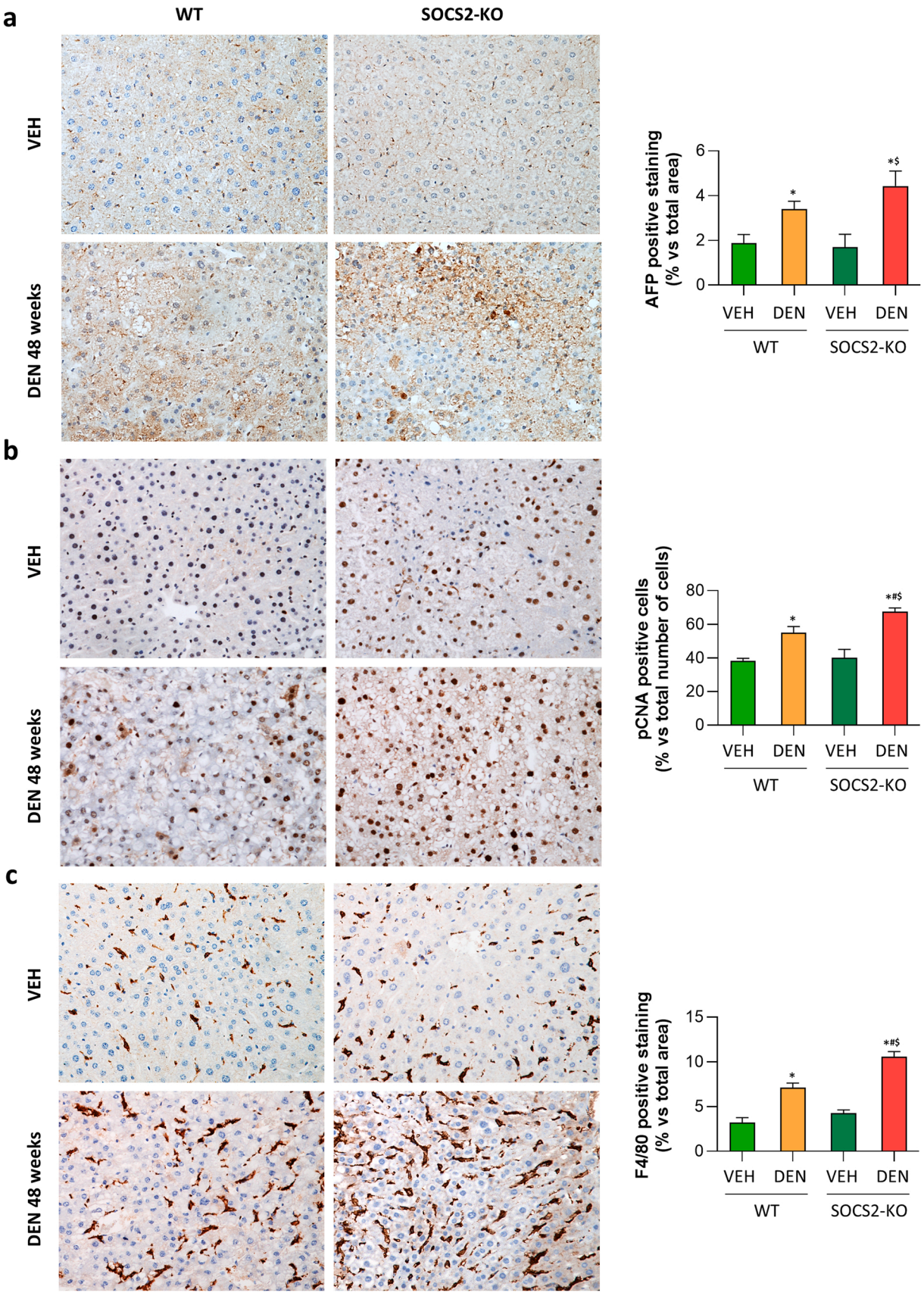

(caption on next page)

Fig. 3. Lack of SOCS2 increases the marker levels of HCC diagnosis, proliferation, and macrophage detection in DEN-treated mice. WT and SOCS2-KO male mice were given a dose of DEN (25 mg/kg) or VEH at 15 days of age and liver tissues were isolated from mice after 48 weeks, paraffin-embedded and sectioned for staining and quantification. At least 10 fields from different mice were counted. (a) Alpha-Fetoprotein (AFP) expression determined by immunohistochemistry in liver sections of WT (n = 9–10) and SOCS2-KO (n = 15–20) mice 48 weeks after VEH or DEN injection. High power (x20 magnification) representative microscopic pictures (left) and quantification of AFP positive staining expressed as % *vs* total area (right) are shown. (b) Proliferating cell nuclear antigen (pCNA) expression determined by immunohistochemistry in liver sections of WT (n = 9–10) and SOCS2-KO (n = 15–20) mice 48 weeks after VEH or DEN injection. High power (x20 magnification) representative microscopic pictures (left) and quantification of pCNA positive-stained cells expressed as % *vs* total cells (right) are shown. (c) F4/80 macrophage marker expression detected by immunohistochemistry in liver sections of WT (n = 9–10) and SOCS2-KO (n = 15–20) mice 48 weeks after VEH or DEN injection. High power (x20 magnification) representative microscopic pictures (left) and quantification of F4/80 positive staining expressed as % *vs* total area (right) are shown. Bars represent mean values ± SEM within each group. Statistical significance is indicated (* $p < 0.05$ *vs* WT-VEH, # $p < 0.05$ *vs* WT-DEN, $ $p < 0.05$ *vs* SOCS2-KO-VEH).

HCC onset and progression after more than 40 weeks post DEN administration both in WT and other mice genotypes [10,40,47]. Interestingly, although 12 and 24 weeks after HCC induction were not long enough to see significant differences between genotypes in the number of animals studied, sonographies allowed to evaluate the progression of tumor formation without euthanasia. Henceforth, we suggest the use of this method as a minimum-invasive alternative to monitor HCC progression in mice at early time points.

When evaluating differences between genotypes in the physiological and metabolic parameters along the study, it was essential to regard that homozygous $socs2^{-/-}$ mice display gigantism characterized by an increase in body weight and length associated with longer bones and enlargement of most organs, as well as alterations in major urinary protein levels, and thickening of dermal layers [28,39].

As mentioned above, DEN is a potent inducer of liver injury, and its hallmarks are necrosis, inflammation, and hepatocellular damage [40,48]. In addition, HCC livers are known to display profound architectural and functional alterations that give rise to severely perturbed tissue [49]. Consistently, our model revealed substantial modifications in cellular, lobular, and trabecular structures, as well as enhanced numbers of infiltrated leukocytes in response to DEN. Remarkably, all these alterations were significantly worsened in SOCS2-KO mice. This fact can be explained by the regulation that SOCS2 protein exerts on GH/STAT signalling in the liver [28]. DEN induces carcinogenesis after being bioactivated by P4502E1 cytochrome (CYP2E1), among other hepatic enzymes, resulting in the appearance of DNA adducts that trigger oncogenic mutations that contribute to liver cancer progression under proliferative stimulus [50]. GH regulates the expression of CYP2E1 in the liver, therefore DEN bioactivation may be potentiated in the absence of SOCS2. In addition, lack of this protein leads to the uncontrolled activation of the inflammatory signalling mediated by STATs, thus increasing inflammatory cell infiltration in the liver of these mice. Consistently, it has been described that tumor associated macrophages are linked to HCC invasiveness and poor prognosis, which would explain the higher malignancy grade found in DEN-treated SOCS2-KO mice [10]. Furthermore, high levels of serum ALT and AST were observed in tumor bearing mice compared to controls, reflecting that murine liver damage is comparable to the human HCC patients, where an increase of these enzymes is associated with enhanced HCC risk [51].

Hepatic fibrosis is a ubiquitous response to chronic injury of the liver and hepatic cells undergo activation from a quiescent to a proliferative phenotype that synthesises high collagen levels when there is a liver insult [52]. In our model, Sirius red staining was increased in both DEN-treated genotypes compared to non-treated controls, but SOCS2-lacking animals exhibited a stronger fibrosis in liver lesions probably as a response of the enhanced tissue injury already observed in H&E sections. Curiously, as SOCS2 is a key regulator of STAT5 signalling in the liver, one might expect that STAT5 would be the major responsible of driving aggravated fibrosis in SOCS2-KO mice. However, other studies with transgenic mice have reported a protective role of STAT5 in liver fibrosis [53,54]. In our model, where there is a total deficiency of SOCS2, the hyperactivation of STAT5 has been demonstrated in liver tissues. But it is not the unique STAT that is upregulated; also, STAT3 has shown significantly higher phosphorylated levels in DEN-treated SOCS2-KO mice compared to their controls. Therefore, this could explain that not only STAT5 but also STAT3 would be orchestrating the enhanced fibrosis in these animals through the regulation of its target pro-fibrotic genes including *tgfβ* and *collagen1*, among others [53–55].

AFP has long been accepted as a biomarker for clinical liver cancer diagnostic and prognostic analyses [56,57]. This protein is normally found at extremely low levels in the liver of healthy adult animals, as its synthesis is rapidly repressed at birth in the liver and gut [58]. However, it is known to be reactivated in HCC. In our model, the positive AFP staining in both groups of treated mice compared to controls indicate the efficient HCC induction in response to DEN administration. However, and consistently with all our previous data, there was a more marked AFP expression in SOCS2-KO animals corresponding to more advanced liver lesions with a poorer prognosis.

Upon death-induced stimulus, hepatocytes release factors that activate liver resident macrophages and promote the infiltration of circulating monocytes into the liver which activates the inflammatory response [59]. In this regard, an increased accumulation of the cell membrane macrophage marker F4/80 was observed in tumor bearing animals with more marked expression observed in SOCS2 lacking mice. These data synchronise with the observations in H&E mouse liver sections, where significantly more inflammation evidenced by the increased number of inflammatory foci and microgranulomas was observed in knockout mice.

This inflammatory state generated in the liver drives in turn the compensatory proliferation of hepatocytes leading to the initiation and/or progression of HCC development [60]. In addition, exposure to DEN induces hepatocyte death which results in a more intense compensatory proliferative response by the surviving fraction of these cells. Therefore, it was not surprising to find elevated staining levels of pCNA in DEN-treated animals, with even more higher numbers in SOCS2-lacking ones, due to the more aggressive tissue damage and more intense inflammatory response.

This loop of inflammation and uncontrolled proliferation in the liver of DEN-induced HCC is further accompanied by the expression of co-stimulatory molecules including proinflammatory cytokines and chemokines by resident and infiltrated leukocytes that aggravate the disease progression. So, as expected, in our model, DEN treatment significantly up-regulated sets of genes modulating the inflammatory response. Significant differences observed between WT and SOCS2-KO mice can be reasonably explained by the fact that SOCS2 is a key regulator of cytokine signalling and its loss has a deep effect in the dysregulation of these molecules. This has special relevance in the case of IL-6, which elevated levels in the liver are associated with acute and chronic diseases [61]. This cytokine binds directly to the receptor in the membrane of hepatocytes, activating proinflammatory and oncogenic signals *via* the JAK-STAT3 pathway [62]. Because IL-6 is more abundant in the absence of SOCS2, it may own crucial responsibility in the exacerbated inflammatory and oncogenic responses observed in SOCS2-KO tumor bearing mice. In fact, most of the oncogenic mediators found upregulated in this group of mice are key target genes of JAK/STAT signalling [63].

Remarkably, although STAT5 is the main STAT member subjected under SOCS2 regulation, is not the unique; also, STAT3 is under SOCS2 control, and both proteins establish a crosstalk that regulates their level

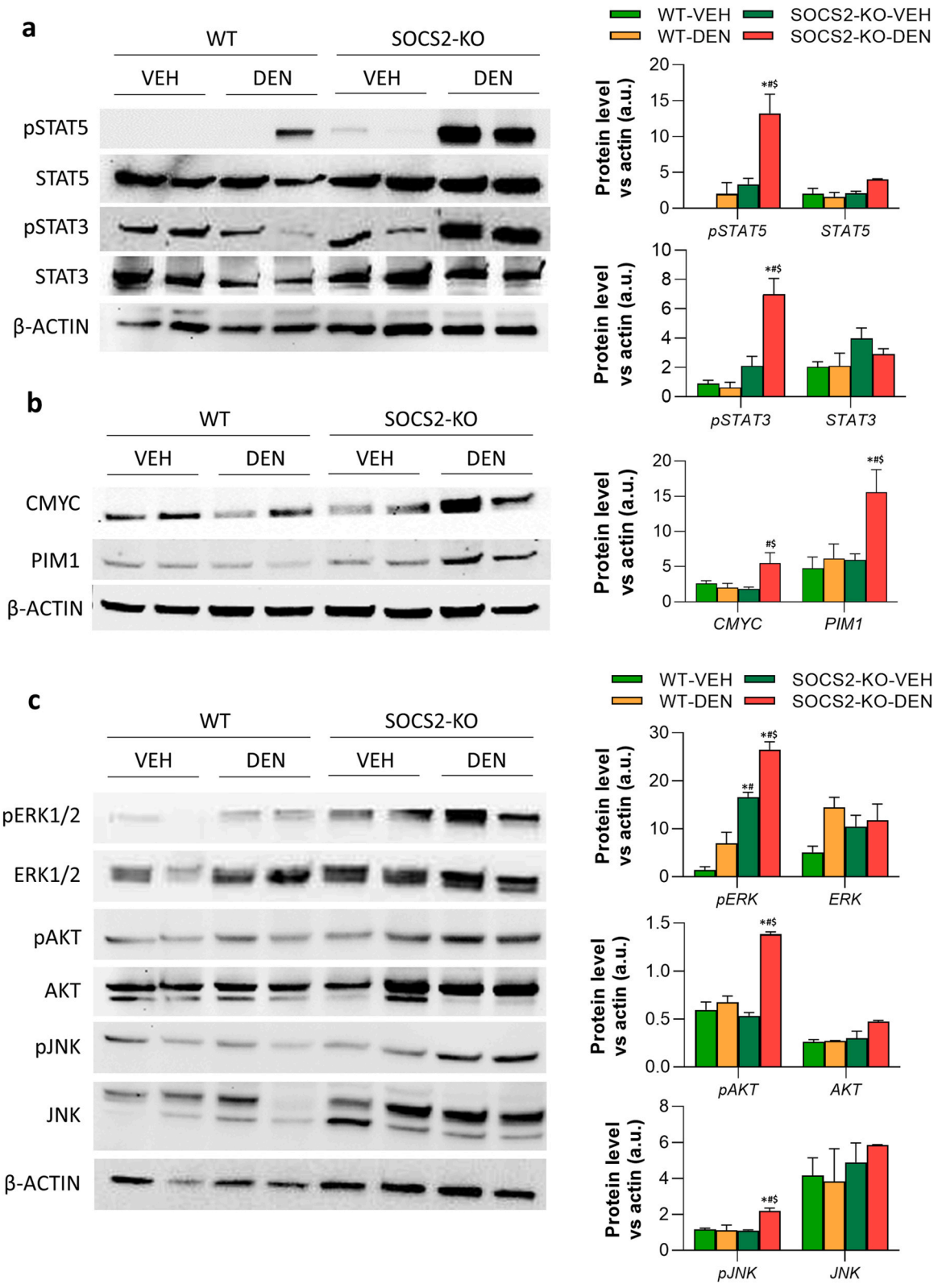

Fig. 4. SOCS2 knockout mice show hyperactivation of inflammatory, oncogenic, and proliferative signalling pathways during HCC. WT and SOCS2-KO male mice were given a dose of DEN (25 mg/kg) or VEH at 15 days of age and liver tissues were isolated from mice after 48 weeks. Total protein from livers was extracted and cell lysates were prepared for Western blotting for phosphorylated antibodies, followed by stripping and re-staining with total antibodies and β-actin as a loading control. Representative images (left) from n = 2–3 independent experiments and protein band quantification (arbitrary units, a.u.) normalized by β-actin (right) are shown for (a) pSTAT5, STAT5, pSTAT3, STAT3; (b) CMYC, PIM1; (**c**) pERK1/2, ERK1/2, pAKT, AKT, pJNK, and JNK antibodies. Bars represent mean values ± SEM within each group. Statistical significance is indicated (* $p < 0.05$ *vs* WT-VEH, # $p < 0.05$ *vs* WT-DEN, $ $p < 0.05$ *vs* SOCS2-KO-VEH).

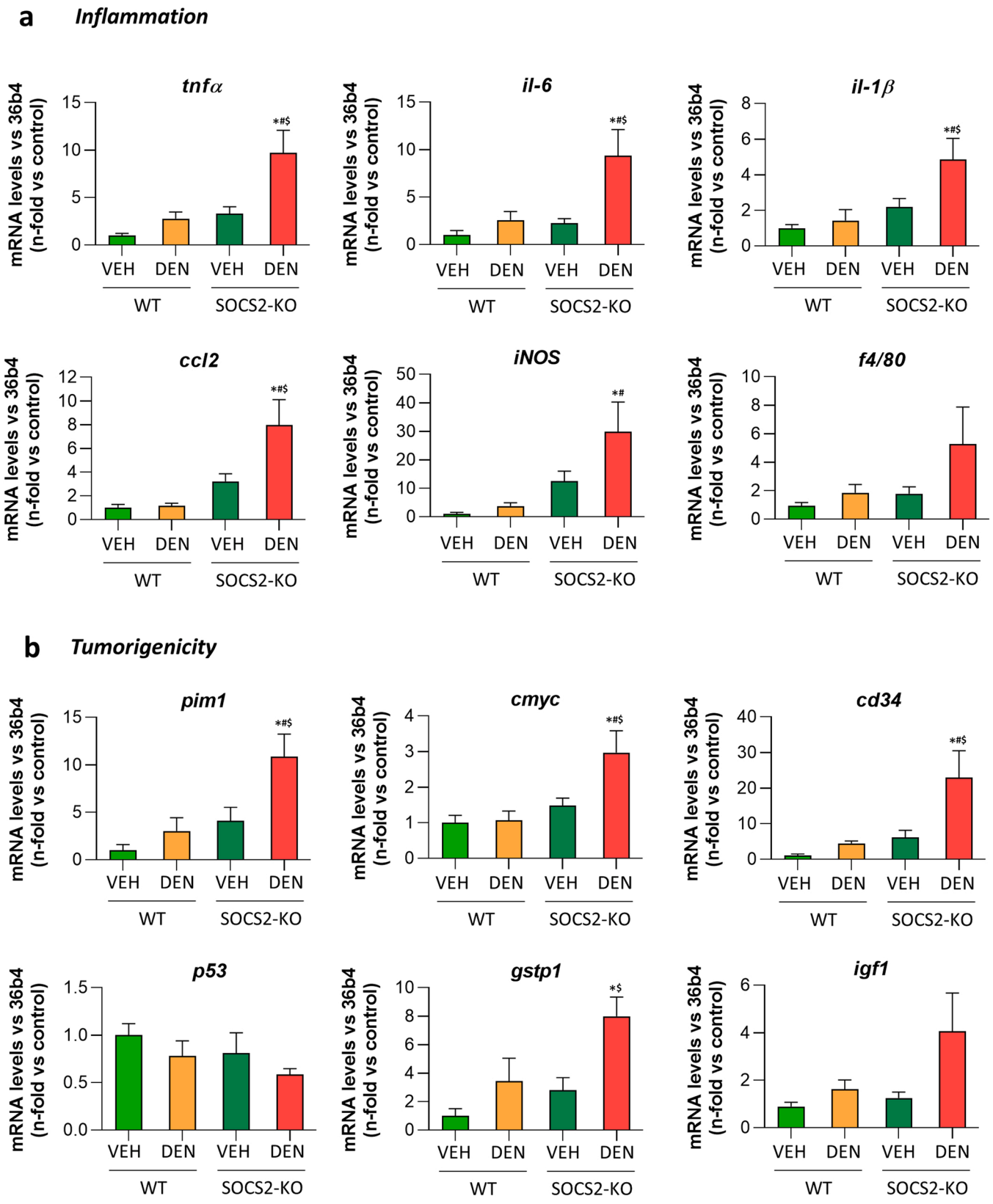

Fig. 5. SOCS2 deficiency enhances the expression of genes involved in inflammatory responses and oncogenic signalling during HCC. WT and SOCS2-KO male mice were given a dose of DEN (25 mg/kg) or VEH at 15 days of age and liver tissues were isolated from mice after 48 weeks. mRNA from livers was extracted and gene expression was analysed by Real-time quantitative PCR. Quantification of mRNA levels (normalized by 36b4 *housekeeping* gene and expressed as fold changes *vs* WT-VEH) of (**a**) the inflammatory mediators *tnfα, il-6, il-1β, ccl2, inos,* and *f4/80*, and (**b**) the oncogenic factors *pim1, cmyc, cd34, p53, gstp1,* and *igf1,* are shown. Bars represent mean values ± SEM within each group. Statistical significance is indicated (* $p < 0.05$ *vs* WT-VEH, # $p < 0.05$ *vs* WT-DEN, $ $p < 0.05$ *vs* SOCS2-KO-VEH).

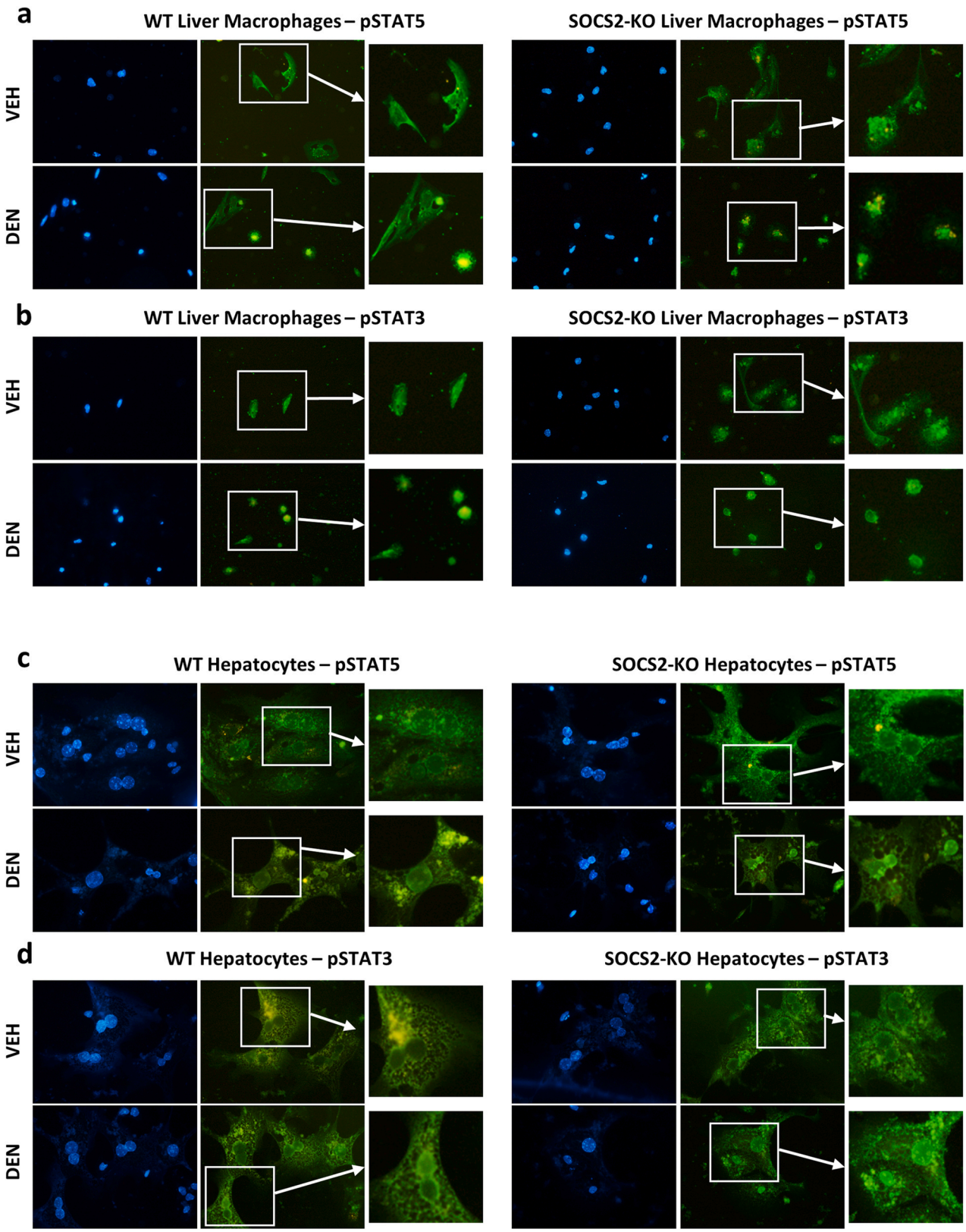

Fig. 6. SOCS2 deletion alters the activation of pSTAT5 and pSTAT3 in liver macrophages and hepatocytes in response to DEN. Cells from total livers from 12 to 15-week-old WT and SOCS2-KO male mice were isolated and separated by gradient into hepatocyte and macrophage populations. Cells were seeded and treated for 24 h with DEN (100 μg/mL) or VEH and subjected to immunofluorescence staining protocol with pSTAT5 and pSTAT3 antibodies. (a, b) Confocal microscopy representative images of (a) pSTAT5 and (b) pSTAT3 in macrophages from WT (left) and SOCS2-KO (right) mice. (c, d) Confocal microscopy representative images of (**c**) pSTAT5 and (**d**) pSTAT3 in liver hepatocytes from WT (left) and SOCS2-KO (right) mice. Images are illustrative of two independent experiments. White arrows indicate detailed augmented images of each condition.

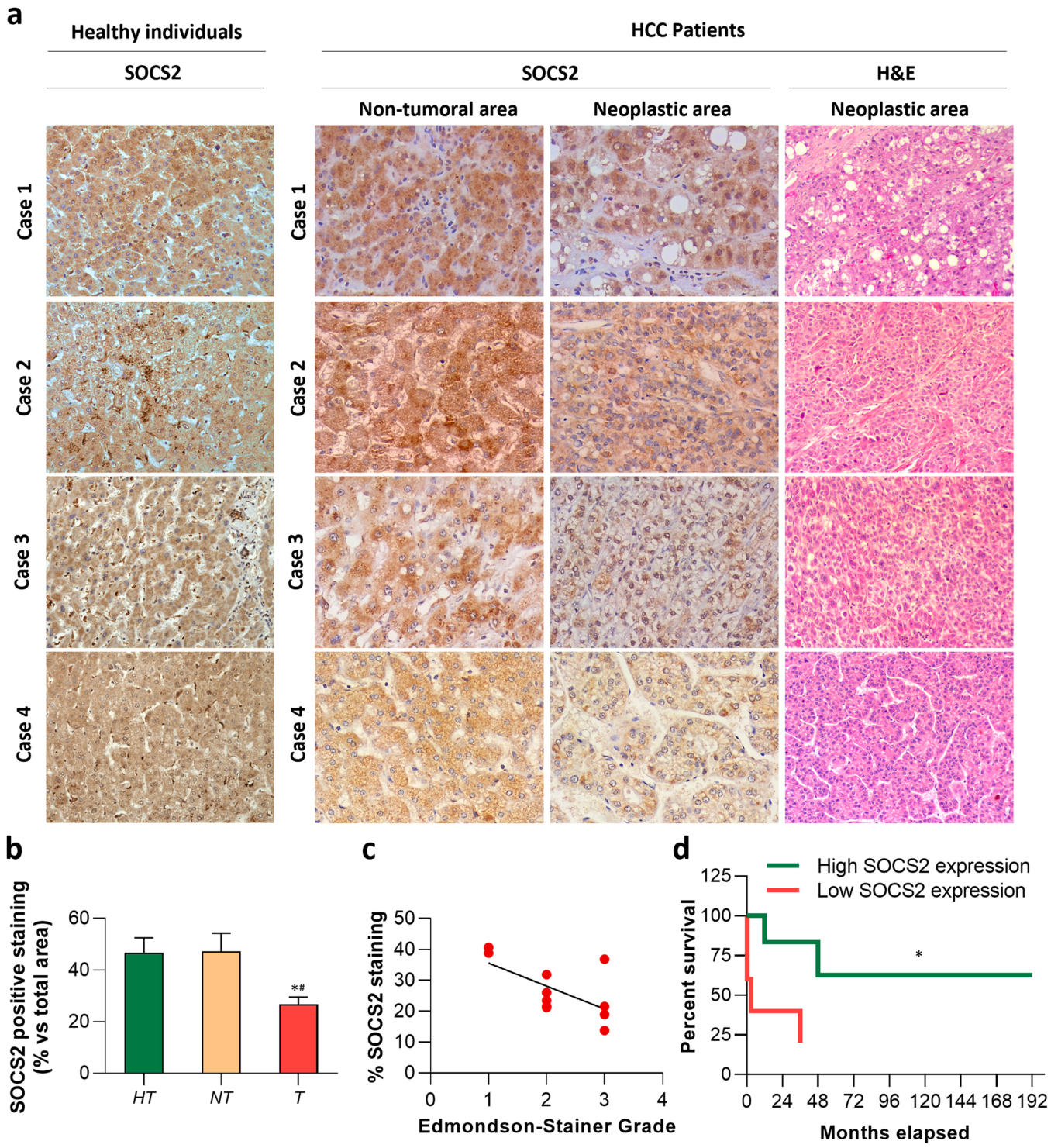

Fig. 7. SOCS2 is a good biomarker of human HCC. Paraffin-embedded livers from human biopsies and autopsies were sectioned, stained, and quantified. At least 10 fields from each sample (case) were evaluated (Edmondson-Stainer Grade in H&E) or counted (SOCS2). (a) Representative images (x20 magnification) of SOCS2 immunohistochemistry of the healthy tissue (left, first column) from healthy individuals (n = 7), the non-tumoral area (middle, second column) and the neoplastic area (middle, third column) from HCC patients (n = 12), and H&E staining of the neoplastic area (right, fourth column) of livers from HCC patients (b) Quantification of SOCS2 positive staining expressed as % *vs* total area. Bars represent mean values ± SEM of each patient/individual. Statistical significance is indicated (* $p < 0.05$ *vs* Healthy tissue, # $p < 0.05$ *vs* Non-tumoral area). Abreviations used: *HT, healthy tissue; NT, Non-tumoral area; T, Tumoral (neoplastic) area.* (**c**) Correlation study between SOCS2 positive staining and Edmondson-Stainer Grade. Plots represent each individual case. (d) Kaplan–Meier analysis of the correlation between SOCS2 positive staining (%) and overall survival in HCC patients. High SOCS2 expression refers to neoplastic areas with 25–50 % positive SOCS2 staining, and low SOCS2 expression to those between 0 % and 25 %. Statistical significance is indicated (* $p < 0.05$ *vs* low SOCS2 expression).

of expression [64]. Indeed, it has been reported that hepatic STAT5 deficiency is linked to compensatory activation of STAT3, which accelerated tumorigenesis in mice [65]. Therefore, it was not surprising to find an up-regulation of both transcription factors when evaluated total protein extracts from DEN-treated SOCS2-KO mouse liver samples. Interestingly, these results were further validated *in vitro* both in hepatocytes and liver macrophages, where DEN exposure triggered an hyperactivation and nuclear translocation of STAT5 and STAT3 that was notably more marked in SOCS2 deficient cells. Furthermore, and considering the close crosstalk between different intracellular signalling pathways, other key molecules involved in cell proliferation and survival, were also affected by SOCS2 deficiency in our model. It is widely known that STAT family members are closely interconnected with ERK, AKT, and other protein kinases, and their expression can depend one to another [66]. Interestingly, activation of ERK and PI3K/AKT has been reported to be concomitant to JAK/STAT activation in HCC cells, and previous studies have demonstrated that JNK activation can induce hepatocyte damage in response to TNFα [67,68]. Hence, our protein expression results only corroborate that SOCS2 deficiency is effectively potentiating the STAT-mediated inflammatory response thereby activating other oncogenic, proliferative, and inflammatory cascades that perpetuate liver tissue damage in HCC mice.

Considering the noiseless and asymptomatic features of HCC during first stages, the prognostic tools existing to assess HCC patient risk remain scarce. Therefore, new strategies are needed based on the identification of new molecules with potential prognostic value [69]. In this sense, we detected the expression levels of SOCS2 protein in tumor, para-tumor, and normal liver tissues in samples from HCC patients and healthy individuals. Very interestingly and clinically relevant, quantifications resulted in a significantly lower expression of this protein in those areas that corresponded to neoplastic regions compared to healthy tissue. Additionally, and concurring with previous studies in gene expression profiles from multiple databases, the correlation analysis showed that SOCS2 protein reduction was significantly correlated with more severe lesions according to Edmondson-Steiner grade [19,70,71]. Furthermore, we found that higher levels of SOCS2 expression are associated to longer HCC patient survival time, as it has also been reported by others [71]. Therefore, our results suggest that SOCS2 is being downregulated in liver neoplasia, which is triggering a more aggressive development of HCC, and that SOCS2 expression is preventing surrounding liver tissue to undergo damage not only in mice but also in human HCC. However, the relatively low number of patient samples that we had access to, limited the performance of a deeper and more extended analysis of the prognostic/diagnostic value of SOCS2 in human HCC.

Collectively, our data suggest that SOCS2 is closely associated with murine and human HCC and its expression prevents liver carcinogenesis through the regulation of STAT5 and STAT3 signalling. These findings may provide useful insight for developing new therapeutic strategies for the treatment and/or prognosis of HCC.

Ethics approval

ULPGC, OEBA-ULPGC 11/2018; CEIm Las Palmas:2021–406–1.

Funding

This research was supported by the “Premios Fundación DISA a la Investigación Biomédica 2019” funded by DISA Foundation, “Ayudas para la financiación de Proyectos de investigación, programa de ayudas ULPGC 2018” funded by the University of Las Palmas of Gran Canaria, and “Ayudas Juan de la Cierva Incorporación 2018” funded by the Ministry of Science and Innovation.

CRediT authorship contribution statement

Juan José Cabrera-Galván: Methodology, Validation, Investigation, Resources. **Eduardo Araujo:** Methodology, Validation, Resources. **Mercedes de Mirecki-Garrido**: Methodology. **David Pérez-Rodríguez:** Methodology. **Borja Guerra:** Conceptualization, Writing. **Haidée Aranda-Tavío:** Methodology. **Miguel Guerra-Rodríguez:** Methodology. **Yeray Brito-Casillas:** Methodology. **Carlos Melián:** Methodology. **María Soledad Martínez-Martín:** Methodology, Resources. **Leandro Fernández-Pérez:** Conceptualization, Resources. **Carlota Recio:** Conceptualization, Methodology, Validation, Investigation, Resources, Formal Analysis, Supervision, Writting, Project admisnistration, Funding acquisition..

Authors contribution

CR, JJCG, EAR, MMG, HAT, MGR, DPR, CM, MSMM and YBC performed the experiments; CR and JJCG analysed the results and made the figures; CR and LF designed the research. CR and BG wrote the paper. All authors provided critical revision of the manuscript.

Consent for publication

Not applicable.

Conflict of interest statement

The authors declare no competing financial interests.

Data Availability

The datasets generated during and/or analysed during the current study are available from the corresponding author on reasonable request.

Appendix A. Supporting information

Supplementary data associated with this article can be found in the online version at doi:10.1016/j.biopha.2022.114060.

References

[1] A. Jemal, F. Bray, M.M. Center, J. Ferlay, E. Ward, D. Forman, CA Cancer J. Clin. 61 (2011) 69.
[2] M. Schlageter, L.M. Terracciano, S. D'Angelo, P. Sorrentino, World J. Gastroenterol. 20 (2014) 15955.
[3] Y.C. Shen, C. Hsu, A.L. Cheng, J. Gastroenterol. 45 (2010) 794.
[4] K.F. Chen, H.L. Chen, W.T. Tai, W.C. Feng, C.H. Hsu, P.J. Chen, A.L. Cheng, J. Pharm. Exp. Ther. 337 (2011) 155.
[5] G. Trinchieri, Annu. Rev. Immunol. 30 (2012).
[6] A. Kuraishy, M. Karin, S.I. Grivennikov, Immunity 35 (2011).
[7] M.N. VanSaun, A.M. Mendonsa, D. Lee Gorden, PLoS ONE 8 (2013).
[8] Q. Lahmar, J. Keirsse, D. Laoui, K. Movahedi, E. van Overmeire, J.A. van Ginderachter, Biochim. Et. Biophys. Acta - Rev. Cancer 1865 (2016).
[9] M.G. Refolo, C. Messa, V. Guerra, B.I. Carr, R. D'alessandro, Cancers 12 (2020).
[10] C. Schneider, A. Teufel, T. Yevsa, F. Staib, A. Hohmeyer, G. Walenda, H. W. Zimmermann, M. Vucur, S. Huss, N. Gassler, H.E. Wasmuth, S.A. Lira, L. Zender, T. Luedde, C. Trautwein, F. Tacke, Gut 61 (2012).
[11] S.N. Udden, Y.T. Kwak, V. Godfrey, M.A.W. Khan, S. Khan, N. Loof, L. Peng, H. Zhu, H. Zaki, Elife 8 (2019).
[12] A. Yoshimura, T. Naka, M. Kubo, Nat. Rev. Immunol. 7 (2007).
[13] E.B. Haura, J. Turkson, R. Jove, Nat. Clin. Pract. Oncol. 2 (2005).
[14] M. Jiang, W. wen Zhang, P. Liu, W. Yu, T. Liu, J. Yu, Front. Immunol. 8 (2017).
[15] B. Schultheis, M. Carapeti-Marootian, A. Hochhaus, A. Weißer, J.M. Goldman, J. v Melo, Blood 99 (2002).
[16] K.D. Sutherland, G.J. Lindeman, D.Y.H. Choong, S. Wittlin, L. Brentzell, W. Phillips, I.G. Campbell, J.E. Visvader, Oncogene 23 (2004).
[17] M.G.M. Khan, A. Ghosh, B. Variya, M.A. Santharam, A.U. Ihsan, S. Ramanathan, S. Ilangumaran, BMC Cancer 20 (2020).
18 M.L. Sobah, C. Liongue, A.C. Ward, Front. Med. 8 (2021).
[19] M. Cui, J. Sun, J. Hou, T. Fang, X. Wang, C. Ge, F. Zhao, T. Chen, H. Xie, Y. Cui, M. Yao, J. Li, H. Li, Tumor Biol. 37 (2016).

[20] J.H. Kim, M.J. Lee, G.R. Yu, S.W. Kim, K.Y. Jang, H.C. Yu, B.H. Cho, D.G. Kim, Exp. Mol. Med. 50 (2018).
[21] S. Haan, Front. Biosci. 8 (2016).
[22] F. Farabegoli, C. Ceccarelli, D. Santini, M. Taffurelli, J. Clin. Pathol. 58 (2005).
[23] M.C. Haffner, B. Petridou, J.P. Peyrat, F. Révillion, E. Müller-Holzner, G. Daxenbichler, C. Marth, W. Doppler, BMC Cancer 7 (2007).
[24] D. Iglesias-Gato, Y.-C. Chuan, P. Wikström, S. Augsten, N. Jiang, Y. Niu, A. Seipel, D. Danneman, M. Vermeij, L. Fernandez-Perez, G. Jenster, L. Egevad, G. Norstedt, A. Flores-Morales, Carcinogenesis 35 (2014) 24.
[25] D. Sonkin, M. Palmer, X. Rong, K. Horrigan, C.H. Regnier, C. Fanton, J. Holash, M. Pinzon-Ortiz, M. Squires, A. Sirulnik, T. Radimerski, R. Schlegel, M. Morrissey, Z.A. Cao, Cancer Biomark. 15 (2015).
[26] E. Letellier, M. Schmitz, K. Baig, N. Beaume, C. Schwartz, S. Frasquilho, L. Antunes, N. Marcon, P. v Nazarov, L. Vallar, J. Even, S. Haan, Br. J. Cancer 111 (2014).
[27] V.A. Newton, N.M. Ramocki, B.P. Scull, J.G. Simmons, K. McNaughton, P.K. Lund, Am. J. Pathol. 176 (2010).
[28] C.J. Greenhalgh, E. Rico-Bautista, M. Lorentzon, A.L. Thaus, P.O. Morgan, T. A. Willson, P. Zervoudakis, D. Metcalf, I. Street, N.A. Nicola, A.D. Nash, L.J. Fabri, G. Norstedt, C. Ohlsson, A. Flores-Morales, W.S. Alexander, D.J. Hilton, J. Clin. Investig. 115 (2005).
[29] J. Liu, Z. Liu, W. Li, S. Zhang, Oncol. Lett. 21 (2021).
[30] L. Shi, X. Shang, K. Nie, Z. Lin, M. Zheng, M. Wang, H. Yuan, Z. Zhu, J. Clin. Pathol. 74 (2021).
[31] X. Qiu, J. Zheng, X. Guo, X. Gao, H. Liu, Y. Tu, Y. Zhang, Mol. Cell. Biochem. 378 (2013).
[32] F. Zadjali, R. Santana-Farre, M. Vesterlund, B. Carow, M. Mirecki-Garrido, I. Hernandez-Hernandez, M. Flodström-Tullberg, P. Parini, M. Rottenberg, G. Norstedt, L. Fernandez-Perez, A. Flores-Morales, FASEB J. 26 (2012) 3282.
[33] R. Monti-Rocha, A. Cramer, P.G. Leite, M.M. Antunes, R.V.S. Pereira, A. Barroso, C. M. Queiroz-Junior, B.A. David, M.M. Teixeira, G.B. Menezes, F.S. Machado, Front. Immunol. 10 (2019).
[34] S. Fruchtman, J.G. Simmons, C.Z. Michaylira, M.E. Miller, C.J. Greenhalgh, D. M. Ney, P.K. Lund, Am. J. Physiol. - Gastrointest. Liver Physiol. 289 (2005).
[35] A.D. Burt, B.C. Portmann, L.D. Ferrel, MacSweeńs Pathology of the Liver, Fifth Edition. (Churchill-Livingstone.Elsevier, 2007).
[36] M. Aparicio-Vergara, M. Tencerova, C. Morgantini, E. Barreby, and M. Aouadi, in Methods in Molecular Biology (2017).
[37] T. Nolan, R.E. Hands, S.A. Bustin, Nat. Protoc. 1 (2006).
[38] F. Heindryckx, I. Colle, H. van Vlierberghe, Int. J. Exp. Pathol. 90 (2009).
[39] D. Metcalf, C.J. Greenhalgh, E. Viney, T.A. Wilison, R. Starr, N.A. Nicola, D. J. Hilton, W.S. Alexander, Nature 405 (2000).
[40] R. Tolba, T. Kraus, C. Liedtke, M. Schwarz, R. Weiskirchen, Lab. Anim. 49 (2015).
[41] R. Masuzaki, T. Kanda, R. Sasaki, N. Matsumoto, K. Nirei, M. Ogawa, S.J. Karp, M. Moriyama, H. Kogure, Cancers (Basel) 14 (2022) 2549.
[42] R. Masuzaki, S. Zhao, M.T. Valerius, D. Tsugawa, Y. Oya, K.C. Ray, S.J. Karp, J. Biol. Chem. 291 (2016).
[43] Y. Liu, Y. Yang, J. Du, D. Lin, F. Li, IUBMB Life 72 (2020).
[44] J.S. Lee, I.S. Chu, A. Mikaelyan, D.F. Calvisi, J. Heo, J.K. Reddy, S.S. Thorgeirsson, Nat. Genet. 36 (2004).
[45] S.S. Thorgeirsson, J.S. Lee, J.W. Grisham, Hepatology 43 (2006).
[46] P. Newell, A. Villanueva, S.L. Friedman, K. Koike, J.M. Llovet, J. Hepatol. 48 (2008).
[47] J. Wu, J. Li, R. Salcedo, N.F. Mivechi, G. Trinchieri, A. Horuzsko, Cancer Res. 72 (2012).
[48] J.M. Henderson, N. Polak, J. Chen, B. Roediger, W. Weninger, J.G. Kench, G. W. McCaughan, H.E. Zhang, M.D. Gorrell, Sci. Rep. 8 (2018).
[49] L.X. Yu, Y. Ling, H.Y. Wang, Npj Precis. Oncol. 2 (2018).
[50] S.K. Jin, H. Wanibuchi, K. Morimura, F.J. Gonzalez, S. Fukushima, Cancer Res. 67 (2007).
[51] S. Chidambaranathan-Reghupaty, P.B. Fisher, and D. Sarkar, in Advances in Cancer Research (2021).
[52] D.Y. Zhang, S.L. Friedman, Hepatology 56 (2012).
[53] D. Kaltenecker, M. Themanns, K.M. Mueller, K. Spirk, T. Suske, O. Merkel, L. Kenner, A. Luís, A. Kozlov, J. Haybaeck, M. Müller, X. Han, R. Moriggl, Cytokine 124 (2019).
[54] A. Hosui, A. Kimura, D. Yamaji, B.M. Zhu, R. Na, L. Hennighausen, J. Exp. Med. 206 (2009).
[55] M.Y. Xu, J.J. Hu, J. Shen, M.L. Wang, Q.Q. Zhang, Y. Qu, L.G. Lu, Biochim. Et. Biophys. Acta - Mol. Basis Dis. 1842 (2014).
[56] T. Chen, X. Dai, J. Dai, C. Ding, Z. Zhang, Z. Lin, J. Hu, M. Lu, Z. Wang, Y. Qi, L. Zhang, R. Pan, Z. Zhao, L. Lu, W. Liao, X. Lu, Cell Death Dis. 11 (2020).
[57] A.H. Wu, S. Sell, Immunol. Ser. 53 (1990).
[58] S. Kreczko, A. Lipska, J. Wysocka, Pol. Merkur Lek. 8 (2000).
[59] Z. Shan, C. Ju, Front. Immunol. 11 (2020).
[60] S. Maeda, H. Kamata, J.L. Luo, H. Leffert, M. Karin, Cell 121 (2005).
[61] K. Yamaguchi, Y. Itoh, C. Yokomizo, T. Nishimura, T. Niimi, H. Fujii, T. Okanoue, T. Yoshikawa, Lab. Investig. 90 (2010).
[62] D. Schmidt-Arras, S. Rose-John, J. Hepatol. 64 (2016).
[63] L.N. Heppler, D.A. Frank, Trends Cancer 3 (2017).
[64] S. Igelmann, H.A. Neubauer, G. Ferbeyre, Cancers 11 (2019).
[65] D. Kaltenecker, M. Themanns, K.M. Mueller, K. Spirk, N. Golob-Schwarzl, K. Friedbichler, L. Kenner, J. Haybaeck, R. Moriggl, Cytokine 124 (2019).
[66] L.A. Winston, T. Hunter, Curr. Biol. 6 (1996).
[67] H. Kamata, S.I. Honda, S. Maeda, L. Chang, H. Hirata, M. Karin, Cell 120 (2005).
[68] N.K. Saxena, D. Sharma, X. Ding, S. Lin, F. Marra, D. Merlin, F.A. Anania, Cancer Res. 67 (2007).
[69] S. Tellapuri, P.D. Sutphin, M.S. Beg, A.G. Singal, S.P. Kalva, Indian J. Gastroenterol. 37 (2018).
[70] Z. Yang, H. Zhu, L. Zhang, Q. Wei, L. Zhou, X. Xu, P. Song, J. Liu, H. Xie, S. Zheng, Mol. Biol. Rep. 47 (2020).
[71] E. Lai, Y. Tai, J. Jiang, C. Zhao, Y. Xiao, X. Quan, H. Wu, J. Gao, J. Cell. Mol. Med. 25 (2021).